J|A|C|S
ARTICLES
Published on Web 08/05/2006

van der Waals Interactions and Decrease of the Rotational Barrier of Methyl-Sized Rotators: A Theoretical Study

Jerome Baudry

Contribution from the School of Chemical Sciences, University of Illinois at Urbana-Champaign, Urbana, Illinois 61801

Received January 31, 2006; E-mail: jerome@scs.uiuc.edu

Abstract: Rotational barriers of methyl-sized molecular rotators are investigated theoretically using ab initio and empirical force field calculations in molecular models simulating various environmental conditions experienced by the molecular rotors. Calculations on neopentane surrounded by methyl groups suggest that the neopentane's methyl rotational potential energy barrier can be reduced by up to an order of magnitude by locating satellite functional groups around the rotator at a geometry that destabilizes the staggered conformation of the rotator through van der Waals repulsive interactions and reduces the staggered/eclipsed relative energy difference. Molecular mechanics and molecular dynamics calculations indicate that this barrier-reducing geometry can also be found in molecular rotators surface mounted on graphite surfaces or carbon nanotube models. In these models, molecular dynamics simulations show that the rotation of methyl-sized functional groups can be catalyzed by van der Waals interactions, thus making very rigid rotators become thermally activated at room temperature. These results are discussed in the context of design of nanostructures and use of methyl groups as markers for microenvironmental conditions.

Introduction

Small- to medium-sized molecular rotors have important functional and analytical applications in chemistry. Molecular rotors found in nanoscale assemblies such as in molecular propellers have been receiving particular attention as they are potential building blocks in the design of nanoengines (see ref 1 for a review of such approaches and of the state of the field). Recent experimental and/or theoretical landmark achievements in the design of nanoengines involve large azimuthal[2,3] or altitudinal[4] nanorotors mounted on metallic surfaces. Smaller molecular rotors are involved in the design of crystalline molecular machines (see ref 5 for a review), such as molecular gyroscopes in solid state,[6] and have applications in crystal engineering and design.[7] In addition, smaller molecular rotors are known to be important markers of the micro-environment of the rotator. For instance, modifications of fluorescent molecular rotor's rotational barriers due to changes in the rotor's environment lead to measurable fluorescence quantum yield variations.[8,9] In solid state, methyl groups' rotational dynamics and variations of the methyl's rotational barrier are coupled to modifications of the nonbonded interactions experienced by the rotor.[10−12]

The structural basis of molecular rotors' function is the rotation of the rotator (rotary unit that experiences motion) around the rotor's axle, and the corresponding effective rotational energy barrier is a combination of internal (within the rotor) and environmental (nonbonded interactions) contributions. A more crowded environment around a rotator often leads to steric hindrances increasing rotational barriers with respect to the gas-phase barriers. For instance, barrierless rotators, such as groups attached to sp hybridized carbon atoms forming a triple bond, can experience nonbonded steric hindrances that increase rotational barriers from less than ∼0.6 kcal/mol[13−15] to values significantly above the thermal energy level.[6] Rotational barriers of surface-mounted rotators or "external gear" nanosystems can increase by up to an order of magnitude when the rotator becomes engaged in contact with neighboring rotors.[3,16] Rotational barriers of molecular rotors substituted with halogen atoms increase linearly with the van der Waals radii of the halogen

(1) Kottas, G. S.; Clarke, L. I.; Horinek, D.; Michl, J. *Chem. Rev.* **2005**, *105*, 1281−1376.
(2) van Delden, R. A.; ter Wiel, M. K. J.; Pollard, M. M.; Vicario, J.; Koumura, N.; Feringa, B. L. *Nature* **2005**, *437*, 1337−1340.
(3) Gimzewski, J. K.; Joachim, C.; Schlittler, R. R.; Langlais, V.; Tang, H.; Johannsen, I. *Science* **1998**, *281*, 531−533.
(4) (a) Zheng, X.; Mulcahy, M. E.; Horinek, D.; Galeotti, F.; Magnera, T. F.; Michl, J. *J. Am. Chem. Soc.* **2004**, *126* (14), 4540−4542. (b) Horinek, D.; Michl, J. *Proc. Natl. Acd. Sci. U.S.A.* **2005**, *102*, 14175−14180.
(5) Garcia-Garibay, M. A. *Proc. Natl. Acd. Sci. U.S.A.* **2005**, *102*, 10771−10776.
(6) Godinez, C. E.; Zepeda, G.; Mortko, C. J.; Dang, H.; Garcia-Garibay, M. A. *J. Org. Chem.* **2004**, *69*, 1652−1662.
(7) Karlen, S. D.; Khan, S. I.; Garcia-Garibay, M. A. *Crystal Growth Des.* **2005**, *5*, 53−55.
(8) Iwaki, T.; Torigoe, C.; Noji, M.; Nakanishi, M. *Biochemistry* **1993**, *32*, 7589−7592.
(9) Sawada, S.; Iio, T.; Hayashi, Y.; Takahashi, S. *Anal. Biochem.* **1992**, *204*, 110−117.
(10) Nair, S.; Dimeo, R. M.; Neumann, D. A.; Horsewill, A. J.; Tsapatsis, M. *J. Chem. Phys.* **2004**, *121*, 4810−4819.
(11) Alvarez, F.; Alegría, A.; Colmenero, J.; Nicholson, T. M.; Davies, G. R. *Macromolecules* **2000**, *33*, 8077−8084.
(12) Hayward, R. L.; Middendorf, H. D.; Wanderlingh, U.; Smith, J. C. *J. Chem. Phys.* **1995**, *102*, 5525−5541.
(13) Saebø, S.; Almlöf, J.; Boggs, J. E.; Stark, J. G. *J. Mol. Struct. (THEOCHEM)* **1989**, *200*, 361−373.
(14) Sipachev, V. A.; Khaikin, L. S.; Grikina, O. E.; Nikitin, V. S.; Trætteberg, M. *J. Mol. Struct.* **2000**, *523*, 1−22.
(15) Godinez, C. E.; Zepeda, G.; Garcia-Garibay, M. A. *J. Am. Chem. Soc.* **2002**, *124*, 4701−4707.
(16) Iwamura, H.; Mislow, K. *Acc. Chem. Res.* **1988**, *21*, 175−182.

10.1021/ja060731k CCC: $33.50

substituents,[17] exemplifying the influence of steric interactions on rotator's barrier of rotation.

However, not all condensed environments lead to increased rotational barriers. Theoretical studies of methyl groups' rotations in crystalline state alanine dipeptide and in specific protein environments[18] suggested that methyl groups' rotational barriers can be reduced by about 1 kcal/mol with respect to gas-phase barriers, because of van der Waals interactions that destabilize the methyl group's staggered conformation. A comparable decrease of methyl groups' rotational barriers in solid phase (when compared to the isolated species) has been also suggested to take place in specific environmental conditions in crystalline peptides[19] where the rotational barrier of alanine's side-chain methyl group is reduced by ~30% in the crystal, down to ~3 kcal/mol, and crystalline alkane chains/organic systems[20] where the average methyl group rotational barrier in the crystal is reduced by about 25% of its gas-phase value to ~2.5 kcal/mol. Investigations of methyl's molecular barriers in glassy polymer show that the barrier of the methyl group in the polymer may also be lower than in the monomer unit.[11] In the latter case,[11] the values of methyl rotational barriers were found to be distributed around an average value that is characteristic of the state of the polymer. While the average methyl rotational barrier in the polymer is shifted toward higher frequencies than in the monomer unit, some of the barriers in the polymer could be ~50% lower than in the monomer unit, down to ~0.99 kcal/mol. These results suggests that short-range nonbonded interactions in specific geometries may lead to a decrease of small rotators' rotational barriers. These reduced methyl rotational barriers in condensed phase are somehow counterintuitive as they do not originate from increased free volume and reduced steric clashes around the rotator but, on the contrary, originate from a rather crowded environment.

The goal of the present work is to identify theoretically, using quantum mechanical and empirical force field calculations, optimal molecular geometries that may favor such environment-induced rotations of methyl-sized rotors. The present article focuses first on a simple model system consisting of neopentane surrounded by three methane molecules. Next, calculations on functionalized graphite surfaces and carbon nanotube models are performed to investigate similar barrier-reducing environments in systems larger than the neopentane/methane model.

Methods

Neopentane Model. A model system consisting of neopentane surrounded by three methyl molecules was built as shown in Figure 1 to investigate the rotational potential of the neopentane's central methyl group. Empirical force field (MMFF94s,[21] using the MOE program[22]) and ab initio (using the Spartan program[23]) potential rotational energy barriers as a function of the C(methane)−C(neopentane) distances were calculated at several levels of theory as described in the Supporting Information.

Functionalized Graphite and Carbon Nanotube Models. The rotational barrier of a trichloromethyl rotor was investigated in functionalized graphite (Figure 2) and carbon nanotube (Figure 3) models using an empirical force field (MMFF94s) as described in the Supporting Information. The potential of mean force (ΔA, free energy along the reaction coordinate) of the trichloromethyl's rotation in the nanotube model was calculated from molecular dynamics simulation as described in the Supporting Information.

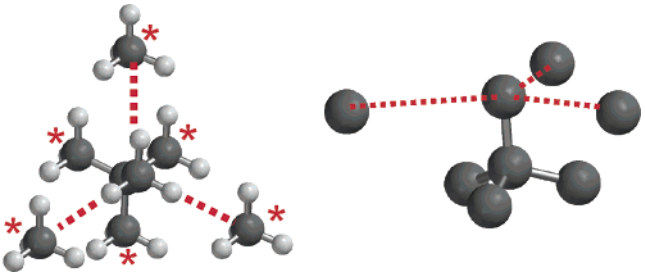

Figure 1. Neopentane/methane model used in both ab initio and empirical force field calculations. Carbon atoms indicated by a red star were held fixed during the energy minimization calculations. Red lines show the C−H directions corresponding to the staggered central methyl group, along which the satellite methane molecules were located. (Left) Top view. (Right) Side view (hydrogen atoms omitted).

Results

Neopentane Model. Figure 4 shows the relative adiabatic potential energy profiles for HF/3-21G* calculations around the central neopentane methyl group for different values of the carbon(neopentane)/carbon(methane) distances ("$C_{(N)}-C_{(M)}$ distances") as defined in Figure 1. The energy profiles calculated for $C_{(N)}-C_{(M)}$ distances of 5.5 and 5 Å are identical and exhibit a three-fold symmetry with maxima corresponding to the eclipsed conformations of the methyl group, i.e., at 0° and −120°, and minima corresponding to the staggered methyl conformations, i.e., −180° and −60°. The 4.7 kcal/mol barrier calculated for these "long" $C_{(N)}-C_{(M)}$ distances is in very good agreement with the gas-phase value of 4.8 kcal/mol indicated in the literature for the same rotation.[24]

When methane molecules are brought closer to the neopentane's central methyl up to a 3.5 $C_{(N)}-C_{(M)}$ Å distance, maxima and minima are located at the same dihedral angle values as for long $C_{(N)}-C_{(M)}$ distances, but the rotational barriers decrease. At a 3.5 Å $C_{(N)}-C_{(M)}$ distance, the barrier is at its lowest value among all the distances considered here. For $C_{(N)}-C_{(M)}$ distances shorter than 3.5 Å, barrier heights increase again, and the rotational potentials exhibit a three-fold symmetry with maxima located at −180° and −60°, (eclipsed conformation), and minima at −120° and 0° (staggered conformation), i.e., in phase opposite to the profiles calculated for $C_{(N)}-C_{(M)}$ distances longer than 3.5 Å.

Figure 5 summarizes graphically the barriers' heights calculated from higher levels of theory than shown in Figure 4 as well as using an empirical force field. The calculated barriers are overall very similar. DFT calculations yield a slightly lower barrier than other methods at "long" $C_{(N)}-C_{(M)}$ distances but yield similar results at lower $C_{(N)}-C_{(M)}$ values. The empirical force field calculations yield higher barriers than the ab initio calculations at short $C_{(N)}-C_{(M)}$ distances but are otherwise very similar to the ab initio results at long $C_{(N)}-C_{(M)}$ distances, in particular when compared to HF/6-31G* calculations (reflecting the parametrization of the force field). At 3.5 Å $C_{(N)}-C_{(M)}$

(17) Toyota, S.; Yamamori, T.; Makino, T.; Oki, M. *Bull. Chem. Soc. Jpn.* **2000**, *73*, 2591−2597.
(18) Baudry, J.; Smith, J. C. *J. Phys. Chem. B* **2005**, *109*, 20572−20578.
(19) Kitson, D. H.; Hagler, A. T. *Biochemistry* **1988**, *27*, 7176−7180.
(20) Morelon, N.; Kneller, G. R.; Ferrand, M.; Grand, A.; Smith, J. C.; Bée, M. *J. Chem. Phys.* **1998**, *109*, 2883−2894.
(21) Halgren, T. A. *J. Comput. Chem.* **1999**, *20*, 720−729.
(22) *Molecular Operating Environment*, version 2005−09; Chemical Computing Group: Montreal, Quebec, Canada.
(23) *Spartan*, version 04/1.0.3; Wavefunction Inc.: Irvine, CA.
(24) Aston, J. G. *Discuss. Faraday Soc.* **1951**, *10*, 73−79.

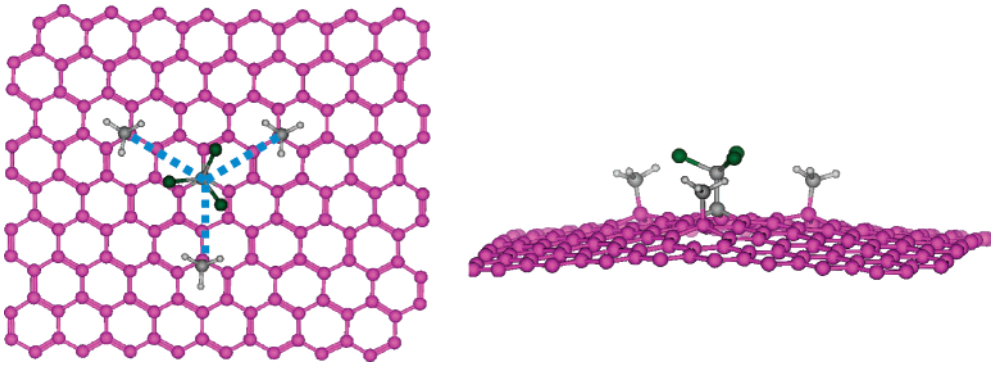

Figure 2. Graphite surface model. (Purple) Carbon atoms from the surface; (gray) carbon atoms from the functionalizing groups; (green) chlorine atoms. Blue lines indicate the C−Cl directions corresponding to staggered trichloromethyl group along which the satellite methyl groups were added. (Left) Top view. (Right) Side view.

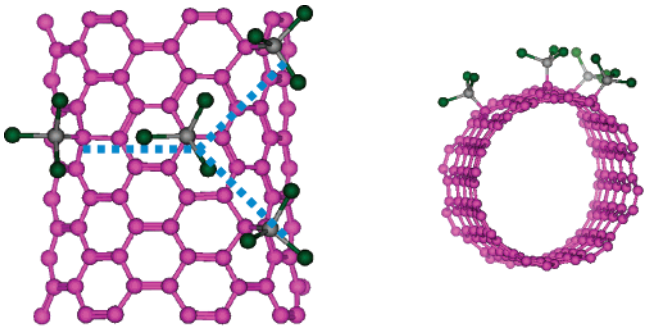

Figure 3. Carbon nanotube model. (Purple) Carbon atoms. (Gray) Carbon atoms from the functionalizing groups. (Green) Chlorine atoms. Blue lines indicate the C−Cl directions corresponding to staggered trichloromethyl group along which the satellite methyl groups were added. (Left) Top view. (Right) Side view.

distances, both ab initio and empirical force field rotational barriers are significantly lower than those calculated for long $C_{(N)}-C_{(M)}$ distance, and also significantly lower than the 2.7 kcal/mol barrier for gas-phase methyl rotation in ethane. The lowest rotational barrier values vary between 0.2 and 0.7 kcal/mol, depending on the level of theory of the calculation, i.e., are within kT of each other ($kT \approx 0.6$ kcal/mol at 300 K). Empirical force field calculations reproduce well the geometry (within 0.1 Å) and the energetics (within 0.5 kcal/mol) of the ab initio results.

$\Delta\Delta E$, a measure of the environment-induced barrier reduction, is calculated by taking the absolute value of the difference between the dihedral barrier at one $C_{(N)}-C_{(M)}$ point and the dihedral barrier for the 5.5 Å $C_{(N)}-C_{(M)}$ distance. Maximum $\Delta\Delta E$ and the corresponding $C_{(N)}-C_{(M)}$ distance calculated from Figure 5 are given in Table 1 for the different levels of theory used. Table 1 shows that satellite methyl groups can lower the neopentane's methyl rotational barrier by as much as 4.1 kcal/mol, i.e., to a rotational barrier lower than 1 kcal/mol, reduced to ~15% of its gas-phase value. The effect is maximum between $C_{(N)}-C_{(M)}$ distances of 3.4 to 3.6 Å, i.e. in a narrow 0.2 Å range of fluctuation of the $C_{(N)}-C_{(M)}$ distance.

Figure 6 shows the relative adiabatic rotational barriers calculated from the empirical MMFF94s force field at $C_{(N)}-C_{(M)}$ of 5.5 and 3.6 Å (maximum of the barrier reduction effect). The 5.5 Å $C_{(N)}-C_{(M)}$ barrier originates essentially from the additive contributions of the van der Waals, dihedral, and bond stretching terms of the potential energy function. The 3.6 Å $C_{(N)}-C_{(M)}$ barrier shows that van der Waals contribution, originating from steric interactions with the satellite functionalization groups, largely cancels the rotator's dihedral contribution and decreases the total potential rotational barrier. The "bond" term is similar to that of the 5.5 Å $C_{(N)}-C_{(M)}$ distance case.

Graphite Surface and Nanotube Models. Figures 7 and 8 show the adiabatic potential energy barriers calculated for a trichloromethyl rotor mounted on graphite (Figure 7) and carbon nanotube (Figure 8) models, with and without satellite methyl functionalization. In both models, the rotational barrier of the central trichloromethyl group is reduced by up to an order of magnitude when satellite groups are present. van der Waals and bond terms, originating from steric interactions between the central rotator and the satellite groups, are in opposite phase with the dihedral term. During the calculations, the distance between the central trichloromethyl's carbon and the surrounding satellite's carbon was found to vary between ~0.2 Å in the graphite model and ~0.25 Å in the nanotube model, i.e in the same range as found in the satellite methyl/neopentane ab initio calculations to induce the maximum barrier-reducing effect.

Figure 9 (top) shows values of the central trichloromethyl's dihedral angle during 1.2 ns molecular dynamics simulations in the carbon nanotube model, with and without satellite functionalization. Without satellite functionalization the central rotator's dihedral angle fluctuates around a constant value, i.e. indicates a nonrotating trichloromethyl on the simulation time scale. In the case of the carbon nanotube model with satellite functionalization, variations of the central rotator's dihedral angle indicate an essentially freely rotating trichloromethyl group at room temperature. The corresponding free energy profile (ΔA) is shown in Figure 9 (bottom), and is very similar to the adiabatic potential energy profile (ΔE) suggesting that in this model the free energy rotational barrier is essentially of an enthalpic origin.

Discussion and Perspective

van der Waals Interactions and Decrease of Methyl Rotational Barrier. The theoretical results presented here suggest that methyl-sized molecular rotors' rotational barriers can be significantly reduced in specific environments. It is not the goal of the present paper to explain these results in the context of electronic details of methyl rotations. Such details

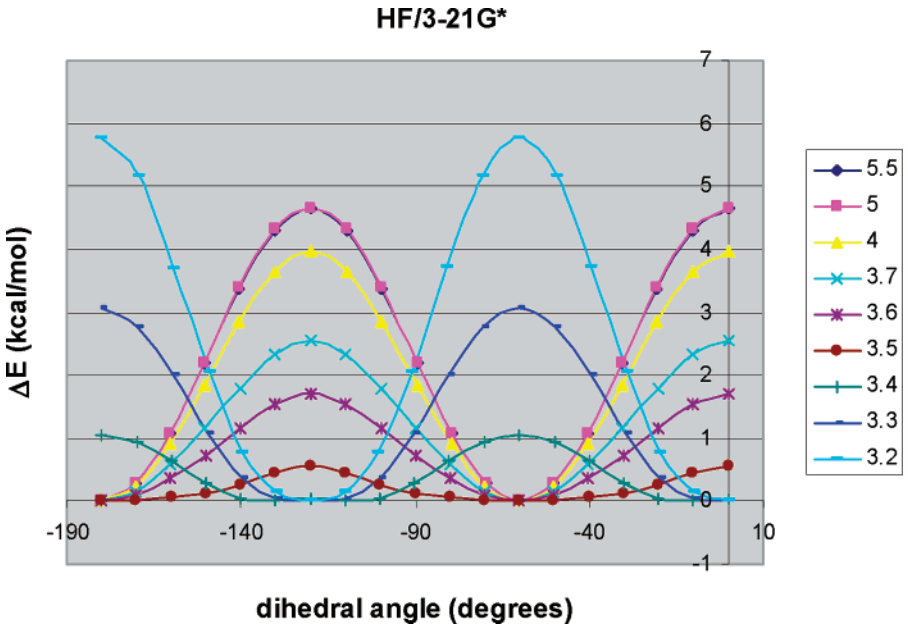

Figure 4. HF/3-21G* ab initio adiabatic potential energy profiles for the central neopentane's methyl group in the neopentane model. The values on the right correspond to the $C_{(N)}-C_{(M)}$ distances used in the ab initio calculations.

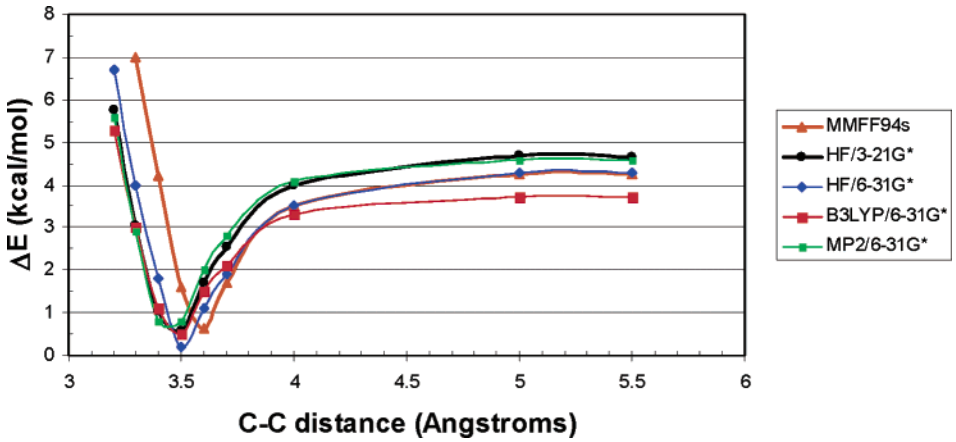

Figure 5. Adiabatic potential energy barriers obtained from ab initio and empirical force field (MMFF94s) calculations in the neopentane model as a function of the $C_{(N)}-C_{(M)}$ distance.

Table 1. Maximum $\Delta\Delta E$ and Corresponding $C_{(N)}-C_{(M)}$ Distances, from Data in Figure 5

	$\Delta\Delta E$ (in kcal/mol)	$C_{(N)}-C_{(M)}$ distance (in Å)
MMFF94s	−3.6	3.6
HF/3-21G*	−4.1	3.5
HF/6-31G*	−4.1	3.5
B3LYP/6-31G*	−3.2	3.5
MP2/6-31G*	−3.8	3.4−3.5

are the subject of discussion, and no mechanism is universally accepted (see ref 25 for a review). In the cases presented here, as also in ref 18, empirical force field calculations reproduce well the ab initio results and suggest that the partial cancellation of the van der Waals and intrinsic dihedral terms leads to a reduced energy difference between the staggered and eclipsed conformations of the methyl groups. The significant contribution of the potential energy function's bond length term observed in Figures 7 and 8 suggests also that in the larger-model systems, the amplitude of the barrier decrease is, to an extent, dependent on the quality of the parametrization of the bond-length term.

Unlike MP2 calculations, the HF and B3LYP calculations performed here do not describe dispersion forces—the attractive part of the van der Waals potential. Figure S1 in Supporting Information shows that for both the eclipsed and staggered central methyl conformations, the $C_{(N)}-C_{(M)}$ distances at which the methyl rotational barrier is the lowest (around 3.5 Å) correspond to the "repulsive part" of the van der Waals interactions, correctly described in HF and B3LYP calculations. Therefore, the ab initio calculations presented here effectively describe well, in the models studied here, the short-range van der Waals interactions suggested by empirical force field calculations to be primarily responsible for the reduced barrier of rotations at the optimum $C_{(N)}-C_{(M)}$ distances.

Is the Rotator's Rotation Catalyzed by van der Waals Interactions? Molecular dynamics calculations in the carbon nanotube model show a greatly increased trichloromethyl's rotational frequency at room temperature when satellite groups

(25) Kundu, T.; Pradhan, B.; Singh, B. *Proc. Indian Acad. Sci.* (*Chem. Sci.*) **2002**, *114*, 623−638.

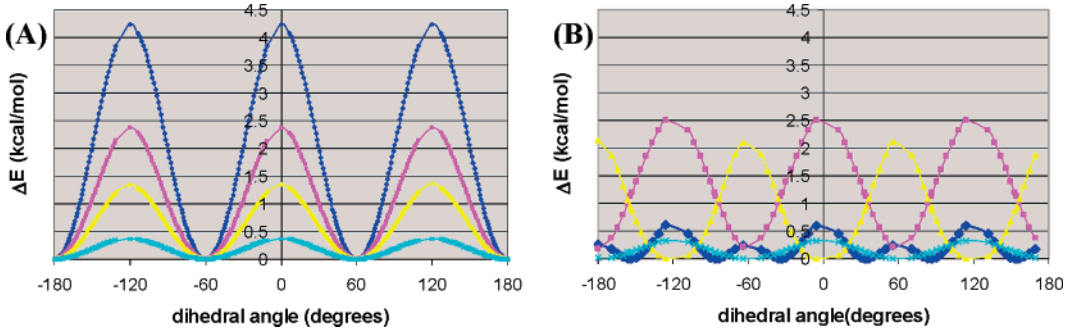

Figure 6. Adiabatic potential energy barriers for the central neopentane's methyl group in the neopentane model (A) $C_{(N)}-C_{(M)}$ distance of 5.5 Å, (B) $C_{(N)}-C_{(M)}$ distance of 3.6 Å. (Blue) Total energy. (Purple) Dihedral contribution. (Yellow) van der Waals contribution. (Cyan) Bond stretch contribution.

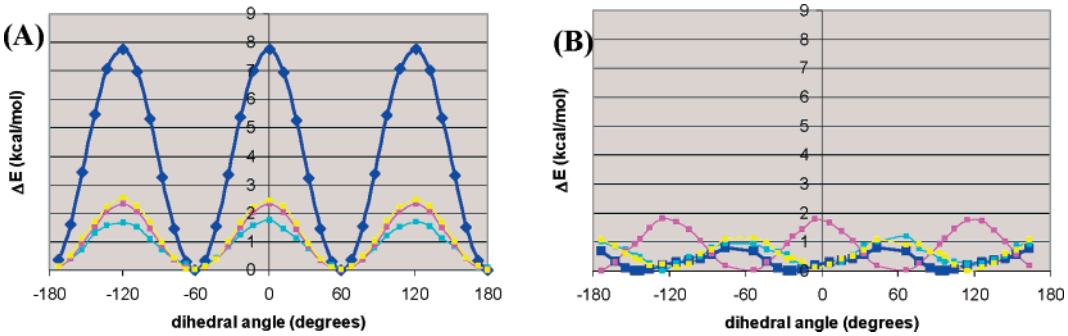

Figure 7. Adiabatic potential energy barrier for the trichloromethyl group from empirical force field calculations in the graphite surface model. (A) Without satellite functionalization. (B) With the methyl group functionalization as indicated in Figure 2. (Blue) Total energy. (Purple) Dihedral contribution. (Cyan) Bond stretch contribution. (Yellow) van der Waals contribution.

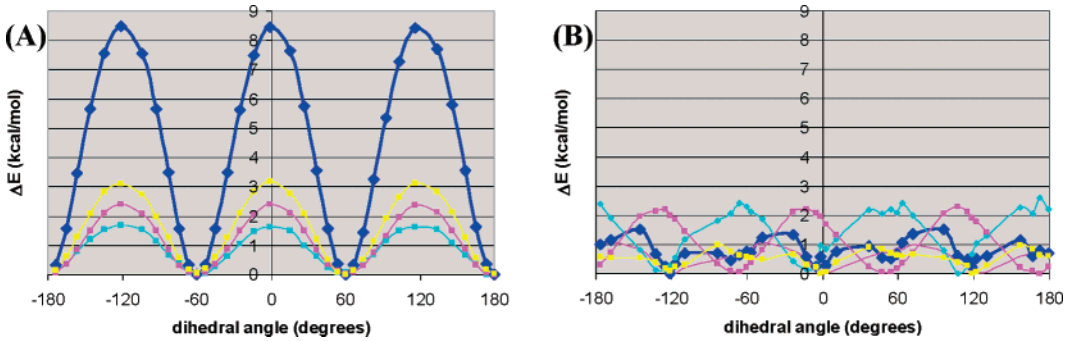

Figure 8. Adiabatic potential energy barrier for the trichloromethyl group from empirical force field calculations in the carbon nanotube model. (A) Without satellite trichloromethyl groups functionalization. (B) With satellite functionalization as shown in Figure 3. (Blue) Total energy. (Purple) Dihedral contribution. (Cyan) Bond stretch contribution. (Yellow) van der Waals contribution.

are present. Approximate rates of rotations at 300 K for the central rotor are calculated (using a simplified rate equation as in ref 19) to be about 600 rotations per 1.2 ns in the case of the carbon nanotube model with satellite functionalization and of 0.005 rotations per 1.2 ns without satellite functionalization, i.e. simulation times in the microsecond time scale are needed to observe rotations without satellite functionalization. These calculated rates are in agreement with the results shown in Figure 9 (top), where no trichloromethyl rotation is visible for the model without satellite functionalization during the simulation time scale. The free energy profile of the corresponding rotation with satellite groups, Figure 9 (bottom), shows low free energy barriers for methyl rotation, very similar to the potential energy profile that is significantly reduced when satellite functionalization is present. As previously proposed in studies of methyl group rotation in crystalline peptides,[18,19] this can be explained by a catalytic effect of the environment on the methyl rotation. Specifically, these results suggest that van der Waals interactions catalyze the rotation of the rotator by decreasing the "transition state barrier", i.e., the rotational barrier of the trichloromethyl group in the present case. Calculations of free energy barriers should be performed whenever possible to investigate such potential catalytic effects, as changes in the methyl's environment upon heating may lead to significant differences between free-energy and adiabatic potential-energy rotational barriers.[18]

Could this Catalytic Effect be Used in Nanodesign? The present results are important to understand a possible structural reason for the decrease of methyl's rotational barriers such as those experimentally observed for instance in glassy polymers[11] or organic crystals,[12,20] or theoretically suggested in crystalline peptides,[18,19] where methyl groups are probes of their local environment. In these cases it would be of particular interest to verify if such a "staggered-destabilizing" geometry can be identified around the methyl groups and are responsible for reduced methyl rotational barriers.

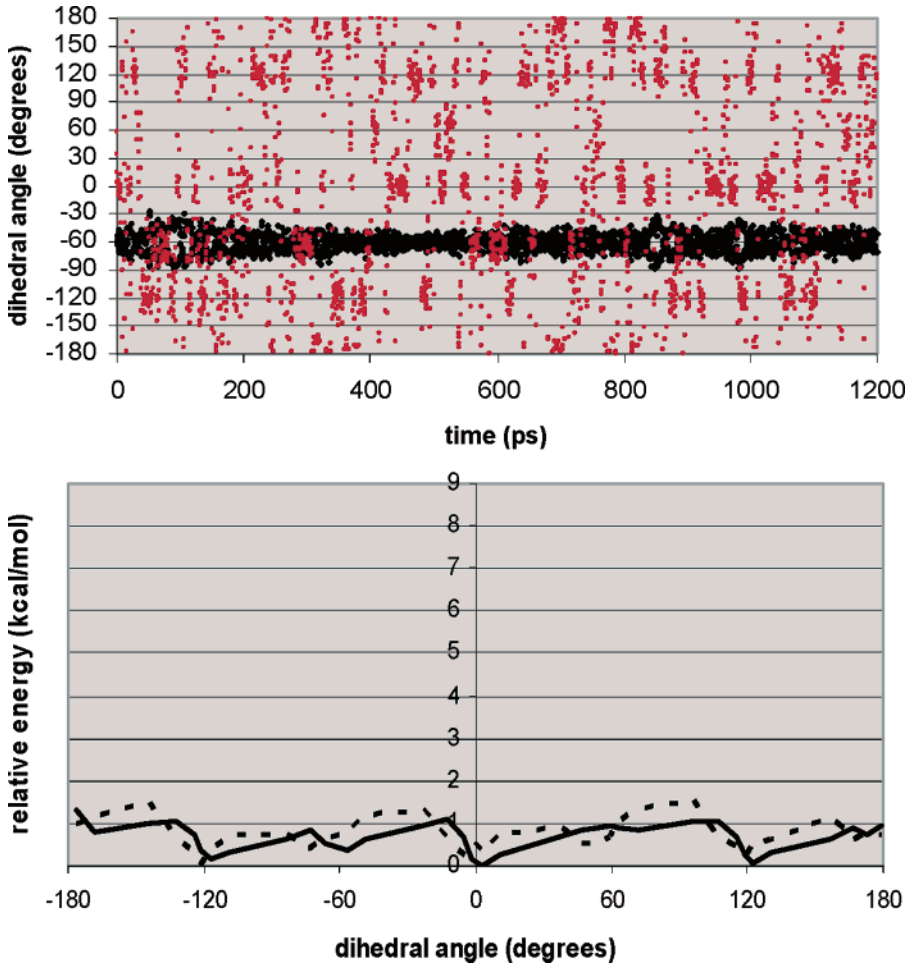

Figure 9. (Top) Time series of the central trichloromethyl group's dihedral angle in the nanotube model without (black) and with (red) trichloromethyl satellite functionalization. (Bottom) Solid line; potential of mean force (free energy, ΔA); dashed line: adiabatic potential energy (ΔE, reproduced from Figure 8B) for the central rotator's rotation in nanotube model with satellite functionalization. Same scale as that of Figure 8.

More generally, the catalytic effect suggested in the present study could have implications in crystal design. Optimization of crystal packing can lead to reduced steric hindrance[26] that may allow freer rotations around the axle. Another possible approach to control the rotator's rotational barrier could be to attempt to reproduce a catalytic effect by modifying the density around the rotator in a controlled way. Although the crystallization process would disrupt idealized geometries, the existence of experimentally verified examples where methyl groups experience decreased rotational barriers in solid phase[11−12,18−20] show that such an effect can be obtained in principle.

However, the present results do not describe nanoengines. The rotators investigated here are small, and their rotations correspond to thermal hopping between energy wells that are neither unidirectional nor controllable. The van der Waals radii of the atoms in the stator and the rotator could be used to guide the design of potential nanorotors with reduced rotational barriers, as suggested in ref 17. For instance, using a central methyl group or central tribromomethyl group instead of trichloromethyl in the graphite surface and carbon nanotube models makes the van der Waals interactions between the satellite groups and the rotator either too hindering or not strong enough to induce a significant catalytic effect. Preliminary results (not shown here) suggest that it may be possible to significantly build up the size of the molecular rotator and design satellite functionalization that leads to reduced barriers of rotations. It will be of interest to investigate what is the maximum rotator size that can be compatible with the proposed van der Waals catalysis of rotation and whether the directionality of rotation can be controlled through, for instance, polarization of the rotator and use of an electric or magnetic field in the model, such as in ref 4b.

Acknowledgment. I thank Jeremy C. Smith and Todd J. Martinez for useful discussions, and Jeffrey S. Moore and James P. Wentz for comments on the manuscript. The School of Chemical Sciences' Computer Center, University of Illinois at Urbana-Champaign is acknowledged for its support.

Supporting Information Available: Computational details for ab initio and empirical force field calculations; details of central methyl geometry and absolute energies (in hartrees) of points in Figure 4; absolute energies of points in Figure 5 and Cartesian coordinates of the corresponding structures. This material is available free of charge via the Internet at http://pubs.acs.org.

JA060731K

(26) Karlen, S. D.; Kahn, S. I.; Garcia-Garibay, M. A. *Crystal Growth and Design* **2005**, *5*, 53−55.